

Can Large Language Models Uncover the Structure of Social Opinions?

Anonymous ACL submission

Abstract

Understanding how opinions on different issues evolve together is essential for modeling collective intelligence, yet this remains under-explored due to the absence of standardized benchmarks. We introduce the concept of an opinion graph, where nodes represent social opinions on real-world events (e.g., presidential elections, stock predictions) and edges capture pairwise relationships between them. Building on this, we present OPINIONBENCH, a new benchmark designed to evaluate whether large language models (LLMs) can uncover the hidden structure within evolving social opinions. Constructed from Polymarket prediction markets, OPINIONBENCH labels event pairs using time-series co-movement, semantic similarity, and metadata, followed by human validation. Experiments show that (1) LLMs consistently outperform baselines in identifying opinion correlations across domains, and (2) LLMs can infer the underlying graph structure through edge prediction. OPINIONBENCH provides a challenging testbed for assessing LLMs' ability to capture complex patterns of social opinion co-evolution.

1 Introduction

Social opinions represent an individual's subjective perspective about uncertain future events—for example, presidential election outcomes, economic trends, or technological breakthroughs. Each person holds a wide range of such opinions shaped by their education, experiences, and social context. These opinions encode people's internal beliefs and expectations about how the world will unfold and serve as the building blocks of collective reasoning and societal decision-making. Social opinions exhibit two key structural features: (1) **Correlation** – Social opinions are not formed or updated in isolation. Multiple opinions are often highly correlated and can shift together when new information emerges. For example, a major poll

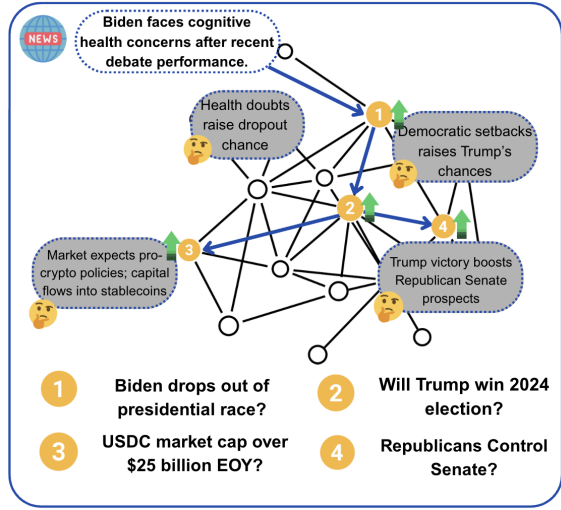


Figure 1: **An example of the opinion graph.** In the opinion graph, each node represents a social opinion (data collected from PolyMarket), and edges denote highly possible reasoning rationale between two social opinions (data constructed with feature design and verified by humans). Similar social opinions are closely correlated with each other and form a graph structure. When the news appears, multiple social opinions in the graph would co-evolve accordingly.

showing a surge in support for Donald Trump may simultaneously update beliefs about “Will Trump win the 2024 election?” and “Will Republicans control the Senate?”, as the two events are tightly connected. Likewise, an unexpected Federal Reserve policy announcement can jointly influence opinions about interest rates and Bitcoin prices, reflecting shared macroeconomic sentiment (Li et al., 2024; Lee et al., 2025; Radivojevic et al., 2024). (2) **Transductivity** – Beyond pairwise edge relationships, if an opinion A is related to B, and B to C, individuals may implicitly associate A with C. Such multi-hop dependencies allow information or belief changes to propagate indirectly across cross-domain opinions (Zhu et al., 2003).

These properties make it natural to represent social opinions using an **opinion graph**. In this graph,

each node corresponds to a specific social opinion toward a real-world event, and each edge represents a relationship between two opinions, such as temporal co-movement, semantic similarity, or causal alignment(Kazemi et al., 2020). Because opinions are often correlated and exhibit transductive dependencies, the resulting graph naturally contains clusters and higher-order structures(Fortunato, 2010), where groups of related opinions cohere into tightly connected subgraphs. This graph-based formulation for social opinions provides a principled way to model how opinions interact locally while also capturing how information can propagate globally through complex multi-hop connections(Hegselmann and Krause, 2002).

Identifying and predicting these latent structures within social opinions is crucial for understanding collective dynamics and forecasting societal change. Structural patterns reveal how shocks can propagate through interconnected opinions, potentially amplifying into large-scale shifts—a “butterfly effect” at the level of public belief. Mapping these structures enables applications such as detecting emerging narratives, anticipating coordinated opinion shifts during crises, modeling systemic financial or political risks, and improving the interpretability of large language models analyzing social behavior (Kolajo et al., 2022; Minnema et al., 2023; Glandt et al., 2021; Wang et al., 2024; Cann et al., 2023; Deng et al., 2021; Peng et al., 2021). This raises a central research question: *Can we leverage LLMs to scalably discover the hidden structure inside a large number of social opinions?* Addressing this question would open up new opportunities for analyzing collective reasoning at unprecedented scale and granularity.

To address this question, we first collect high-quality opinion graphs from SWM (Anonymous, 2025), a dataset compiled from Polymarket¹, a decentralized forecasting platform. Each node corresponds to a specific social opinion toward a real-world event, and each edge is labeled based on a combination of time-series co-movement and semantic similarity, with labels generated automatically and validated against human annotations to ensure reliability. We then apply LLMs to perform pairwise edge prediction, enabling us to reconstruct the entire opinion graph from local edge-level inferences and assess whether models can capture both local correlations and global structural patterns.

Our findings reveal two conclusions: (1) LLMs can accurately predict edges in the opinion graph, consistently outperforming heuristic and neural baselines. For example, GPT-4o achieves QWK scores above 0.52 on Cryptocurrency domain, significantly surpassing all heuristic methods. (2) Beyond local edges, LLMs can also recover the global structure of the opinion graph: the predicted graphs exhibit clustering patterns and structural alignments that closely match the ground truth, indicating that LLMs implicitly capture transductive and higher-order regularities in social opinions.

2 Related Work

Social opinion dynamics. Understanding the dynamics of social opinions associated with real-world events, such as co-occurrence, semantic relevance, or implicit causal links, is fundamental to understanding social dynamics. Cataldi et al. (2010) propose a co-occurrence graph to detect tweet topics. The Whatsup framework (Hettiarachchi et al., 2023) resolves co-occurring events using self-learned word embeddings. TimeBank (Gast et al., 2016) and MATRES (Ning et al., 2018) provide structured datasets for temporal and causal relation extraction. Zhou et al. (2021) introduces a BERT-based model for reasoning over event correlations. In the financial setting, MARKETGPT (Wheeler and Varner, 2024) and PLUTUS (Xu et al., 2024) develop pretrained models for market social opinion understanding. However, many of these studies rely on synthetic setups or structured event representations, limiting their applicability to noisy, ambiguous real-world social opinions. Our work differs by introducing a realistic evaluation task constructed from real-world market data, enabling systematic measurement of LLMs’ ability to identify social opinion correlations under temporal uncertainty and semantic sparsity.

Social reasoning. Prior work uses the term “social reasoning” to refer to tasks like understanding social norms, commonsense interactions, or modeling human mental states. For example, SocKET benchmarks LLMs on social-concept understanding and moral expectations (Choi et al., 2023), while Gandhi & colleagues study mental-state reasoning for theory-of-mind modeling (Gandhi et al., 2024). Other work evaluates LLMs’ understanding of social norms in large-scale benchmark settings, such as the Social Norm dataset (Yuan et al., 2024) and the NormAd cultural adaptability frame-

¹<https://polymarket.com/>

160 work (Rao et al., 2025). Prior work often defines
161 social reasoning through individual or small-group
162 cognition, focusing on human-centric scripts or
163 moral norms. In contrast, we define it as identi-
164 fying meaningful connections between real-world
165 social opinions, capturing co-occurrence, semantic
166 relevance, or implicit causality in different domains.
167 Our task centers on reasoning over collective dy-
168 namics using noisy, unstructured signals (e.g., pre-
169 diction markets), shifting focus from interpersonal
170 commonsense to event-level inference relevant for
171 social science and forecasting.

172 3 Preliminary

173 **Definition of opinion graphs.** We represent the
174 relationships among social opinions using an opinion
175 graph $\mathcal{G} = (\mathcal{V}, \mathcal{E})$, where \mathcal{V} is the set of nodes
176 corresponding to individual social opinions, and
177 \mathcal{E} is the set of edges capturing meaningful ratio-
178 nales between pairs of opinions. This graph pro-
179 vides a unified representation of how collective
180 expectations about different real-world events are
181 connected through semantic, temporal, or causal
182 dependencies.

183 **Social opinions as nodes.** Each node $v \in \mathcal{V}$
184 represents a *social opinion* toward a real-world
185 event $e \in \mathcal{E}$. Formally, a node is defined as
186 $v_e := (q_e, \{p_t^e\}_{t=1}^{T_e})$, where q_e is the natural
187 language description of the event, and p_t^e is the time se-
188 ries of daily market-implied probabilities extracted
189 from Polymarket. This time series reflects the
190 evolving collective belief about the event, while
191 q_e provides semantic context. In our framework,
192 only the textual descriptions are used for model
193 inference, whereas temporal signals are utilized
194 for constructing and validating the ground-truth
195 correlations.

196 **Reasoning rationales as edges.** Each edge
197 $(v_i, v_j) \in \mathcal{E}$ represents a *reasoning rationale* that
198 links two social opinions. A rationale provides a
199 textual explanation describing why the two opin-
200 ions are related, such as shared semantic content
201 or correlated temporal dynamics. In other words,
202 edges encode interpretable relational explanations
203 that justify why two opinions should be connected.
204 Because social opinions are often correlated and ex-
205 hibit transductive dependencies, the resulting opin-
206 ion graph naturally forms clusters and higher-order
207 structures.

208 **Opinion structure prediction task.** The task we
209 defined on the opinion graph aims to reconstruct

210 the structure of the underlying opinion graph \mathcal{G}
211 from observed social opinions \mathcal{V} by evaluating the
212 plausibility of edges between node pairs. Formally,
213 given a set of candidate node pairs $\mathcal{P} \subseteq \mathcal{V} \times \mathcal{V}$,
214 the goal is to learn a scoring function $s : \mathcal{P} \rightarrow \mathbb{R}$,
215 where $s(v_i, v_j)$ quantifies the predicted rationale
216 strength between two social opinions v_i and v_j .
217 High scores correspond to pairs that are strongly
218 connected through semantic, temporal, or causal
219 reasoning, while low scores indicate weak or spuri-
220 ous associations. By applying a threshold τ to the
221 predicted scores,

$$\hat{\mathcal{E}} = \{(v_i, v_j) \in \mathcal{P} \mid s(v_i, v_j) \geq \tau\}, \quad (1)$$

222 We aim to obtain a filtered set of edges that define
223 the predicted opinion graph $\hat{\mathcal{G}} = (\mathcal{V}, \hat{\mathcal{E}})$ that should
224 be as similar as possible with the ground-truth one.

225 4 Constructing the Opinion Graph

226 To benchmark the social opinion correlation task,
227 we construct a dataset based on SWM (Anonymous,
228 2025), derived from Polymarket. In this section,
229 we first explain how social opinion pairs are se-
230 lected, then describe our procedure for collecting
231 ground-truth relationship labels.

232 4.1 Social Opinion Node Collection

233 Not all markets offer informative or reliable signals
234 for social opinion reasoning. To ensure that the
235 included events reflect collective crowd social opin-
236 ions rather than noise, we apply two filters: one
237 based on trading volume, the other on volatility of
238 social opinion movement.

239 **Volume filter.** Markets with very low trading vol-
240 ume are often driven by isolated trades and do
241 not reflect meaningful aggregation of public social
242 opinion. We remove the bottom 25% of events by
243 trading volume within each domain. This helps ex-
244 clude illiquid or inactive markets where probability
245 shifts are unreliable.

246 **Volatility filter.** We require the event to have a suf-
247 ficient probability of movement. A flat probability
248 series provides little statistical signal. By impos-
249 ing a minimum volatility threshold, we ensure that
250 the probability series contains enough variation to
251 make the correlation test meaningful. Details are
252 available in Appendix §C.1.

253 4.2 Reasoning Rationale Edge Collection

254 To construct ground-truth edges for the opinion
255 graph, we adopt a hybrid scoring framework that

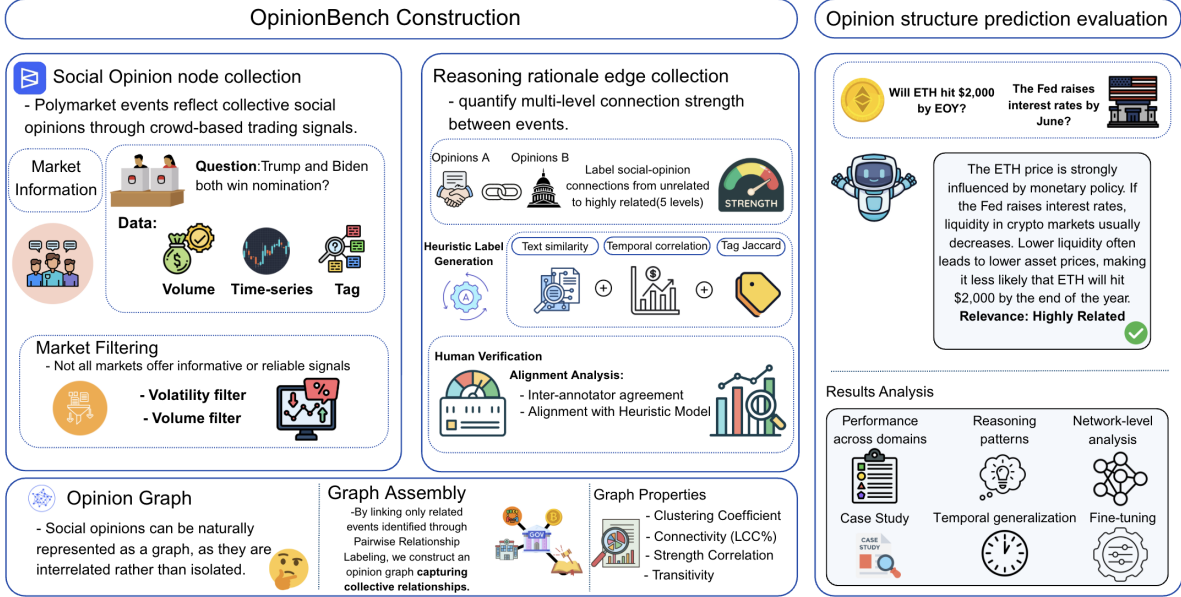


Figure 2: **Overview of the OPINIONBENCH pipeline.** (a) Social opinion node collection from *Polymarket* with market filtering for reliability. (b) Reasoning rationale edge collection quantifies multi-level connections (5 levels) via semantic, temporal, and tag similarities, verified by human annotation. (c) Opinion structure prediction evaluation measures models’ ability to capture opinion relevance across domains, reasoning types, temporal generalization, and network structure.

integrates multiple complementary signals. This approach captures both semantic and temporal aspects of social opinion relationships, allowing us to go beyond surface similarity and identify deeper correlations between event pairs. For each pair (A, B) , we compute four interpretable feature scores, s_1 through s_4 , and combine them into a single composite relevance score.

Feature design. The four features capture distinct yet complementary aspects of social opinion relationships. (1) *Change-point synchrony* s_1 detects statistically significant shifts in each event’s social opinion trajectory and measures how frequently these shifts occur close together in time, capturing coordinated changes in collective expectations. (2) *Tag Jaccard similarity* s_2 compares Polymarket metadata tags, identifying topical overlap and shared discourse contexts. (3) *Minimum time gap* s_3 measures how closely in time the opinion shifts of two events occur, providing a soft measure of temporal proximity. (4) *Textual similarity* s_4 computes embedding-based semantic similarity between event descriptions, capturing lexical and conceptual relatedness beyond metadata. Full details of these feature definitions are provided in Appendix §C.2.

Edge label construction. The four feature scores are linearly combined into a single heuristic cor-

relation score $S(A, B) = \sum_{i=1}^4 \gamma_i s_i(A, B)$. The resulting scores are discretized into five ordinal levels (very weak, weak, medium, strong, very strong), which serve as ground-truth edge labels in our prediction task. By integrating heterogeneous information—temporal dynamics, topical metadata, and textual semantics—this framework produces high-quality, interpretable rationales for edge construction in the opinion graph. We also collect text-based rationale with state-of-the-art LLMs (GPT-4o) as part of the edge attribute.

Human verification. To assess the quality of the heuristic labels, we conduct a human annotation study on a representative subset of 200 event pairs, sampled uniformly across the five correlation levels. Three annotators independently rated each pair based on textual semantics and related news, without access to the underlying time series or model predictions. Inter-annotator agreement was strong, with pairwise Pearson correlations ranging from 0.739 to 0.840 and an intraclass correlation (ICC) of 0.777. Moreover, the aggregated human judgments were well aligned with the heuristic scores, yielding a Pearson correlation of 0.697. These results confirm that the scoring framework reflects intuitive assessments of social opinion correlation. Full details of the protocol and annotation examples are provided in Appendix §I.

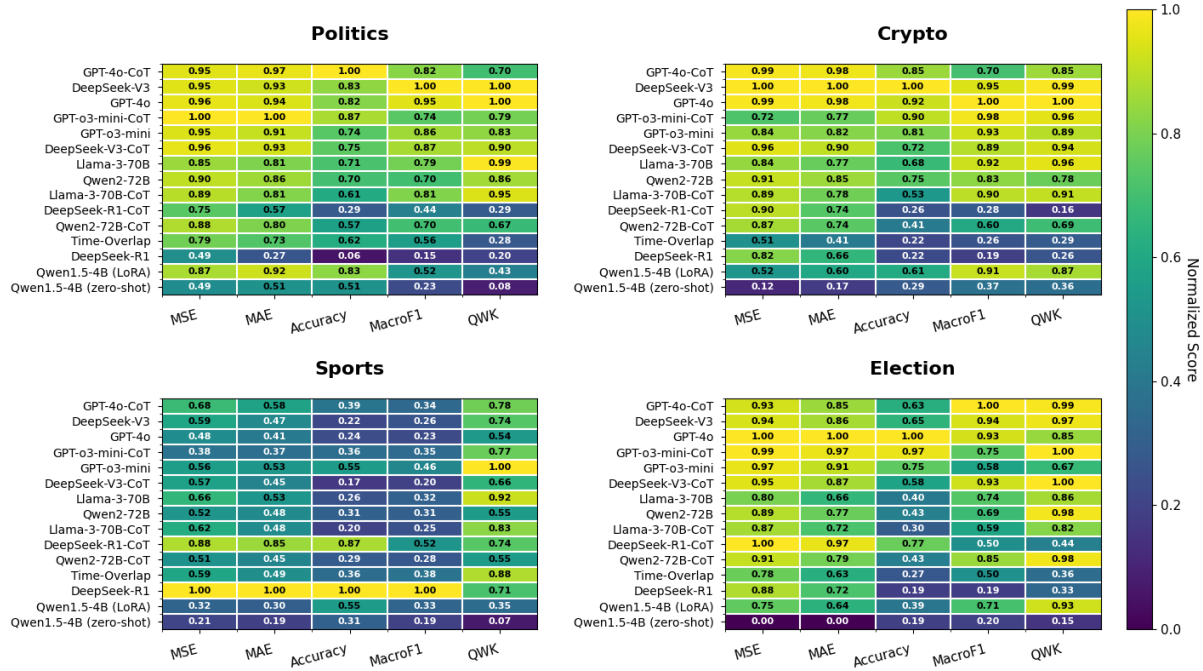


Figure 3: **Performance on opinion graph edge scoring across four domains: Politics, Crypto, Sports, and Election. Only the strongest baseline is included for comparison.** Each heatmap shows model performance across five metrics: MSE, MAE (lower is better before negation), and Accuracy, Macro-F1, QWK (higher is better). To make metrics comparable, error metrics are first negated so that higher values indicate better performance, and then all values are min–max normalized within each metric and dataset. Models are sorted by their average normalized score across all datasets. Higher values indicate better normalized performance.

5 Predicting the Opinion Graph

We use LLMs to perform opinion graph discovery by jointly predicting a *rationale* and a *score* for each candidate edge. Given a pair of social opinions $(v_i, v_j) \in \mathcal{P}$, represented by their event descriptions and opinion trajectories, the model is prompted to reason about their relationship and generate two outputs simultaneously: a textual explanation describing why the two opinions may be correlated, and a scalar score indicating the predicted strength of this relationship. Formally, for each node pair (v_i, v_j) , the LLM implements a mapping $\Phi_{\text{LLM}} : \mathcal{P} \rightarrow \mathcal{R} \times \mathbb{R}$, where \mathcal{R} denotes the space of textual rationales. The output

$$\Phi_{\text{LLM}}(v_i, v_j) = (r_{i,j}, s_{i,j}) \quad (2)$$

consists of a text-based rationale $r_{i,j} \in \mathcal{R}$ explaining the potential connection between v_i and v_j , and a score $s_{i,j} \in \mathbb{R}$ reflecting the predicted strength of their relationship.

The predicted opinion graph is then reconstructed by applying a threshold τ to the set of predicted scores. Specifically, we retain edges with $s_{i,j} \geq \tau$ to form the edge set following Eq. 1, which defines the predicted graph $\hat{\mathcal{G}} = (\mathcal{V}, \hat{\mathcal{E}}_{\mathcal{G}})$.

The generated rationales provide interpretable justifications for each predicted edge, while the scores enable scalable graph recovery through pairwise evaluation. This joint rationale–score prediction framework allows LLMs to explicitly reason about social opinion relationships.

6 Experimental Settings

Baselines. We implement several heuristic baselines that rely on simple similarity or overlap metrics computed from event metadata. We also include a neural baseline using a cross-encoder model ² (`nli-deberta-v3-base`), which computes a scalar relevance score from the concatenated text of the two event descriptions. These continuous scores are then discretized into the same five relevance bins for evaluation.

Prompting-based LLMs. We evaluate models including GPT model family (Hurst et al., 2024), Qwen2 model family (Team et al., 2024), LLaMA model family (Touvron et al., 2023) and DeepSeek-R1 (Guo et al., 2025) using a rationale-based classification setup. Given two social opinion titles and

²<https://huggingface.co/cross-encoder/nli-deberta-v3-base>

descriptions, the LLM first generates a structured rationale explaining links between events, then selects relevance levels. For comparison, we also include a variant where models directly predict the relevance label without explicit reasoning.

Edge-level evaluation metrics. We evaluate performance at both the *edge* and *graph* levels. For edge-level metrics, we include MSE, MAE, Accuracy, Macro-F1, and Quadratic Weighted Kappa (QWK). All of them are aimed for evaluating the classification performance. Typically, QWK is a classical ranking correlation metric computed as

$$\text{QWK} = 1 - \frac{\sum_{i,j} W_{ij} O_{ij}}{\sum_{i,j} W_{ij} E_{ij}}, \quad (3)$$

where O and E are the observed and expected rating matrices, and W is the quadratic weight matrix.

Graph-level evaluation metrics. Graph-level metrics include: (1) Largest Connected Component ratio (LCC), defined as $\text{LCC} = \frac{|V_{\text{max}}|}{|V|}$; (2) Clustering coefficient, $C = \frac{1}{n} \sum_i \frac{2T_i}{k_i(k_i-1)}$, where T_i is the number of triangles through node i ; (3) Strength correlation, $\rho = \text{corr}(s_i^{\text{GT}}, s_i^{\text{Pred}})$, where s_i is the weighted degree; (4) Transitivity, $\text{Trans} = \frac{3 \times \# \text{ triangles}}{\# \text{ connected triples}}$. These metrics jointly assess the global structural fidelity.

7 Experimental Results

LLMs generally achieve strong edge prediction performance across domains. In Figure 3, we evaluate model performance across four domains—Politics, Election, Crypto, and Sports—using both classification (Accuracy, F1, QWK) and regression (MSE, MAE) metrics. Overall, GPT-4o + Chain-of-Thought (Wei et al., 2022) achieves the strongest and most stable results, outperforming smaller variants (e.g., GPT-o3-mini) and competitive open-source baselines (e.g., Meta-Llama-3-70B, Qwen2-72B) in most settings. While minor domain-specific variations exist, the trend highlights that LLMs can effectively infer event relationships from textual descriptions alone, without relying on metadata. Heuristic baselines based on time overlap perform markedly worse, further emphasizing the advantage of language-based reasoning.

Rationale generation helps most in domains requiring complex reasoning. CoT prompting provides the greatest benefit in domains like Politics

Domain	LCC	Clustering	Corr.	Trans.
Politics	92.6 → 82.8	0.088 → 0.087	0.983	78.0% ***
Election	98.5 → 99.3	0.257 → 0.276	0.991	90.8% ***
Crypto	99.4 → 97.8	0.131 → 0.104	0.970	87.8% ***
Sports	91.6 → 45.0	0.077 → 0.034	0.954	90.0% ***

Table 1: **LLM-based predictions preserve network structure.** LCC represents the percentage of the largest connected component ratio. Clustering represents the local cohesion. Corr. represents edge-weight alignment. Trans. represents transitivity. $X \rightarrow Y$ represents the ground-truth one → the predicted one. A small difference between X and Y indicates the high fidelity for prediction. *** indicates $p < 0.05$.

and Election. In these settings, models like GPT-4o-CoT and GPT-o3-mini-CoT achieve notable gains in regression accuracy and ranking consistency, reflecting their ability to uncover indirect dependencies between events. However, these benefits are domain-specific: CoT improves calibration but not classification metrics in Politics, and primarily boosts regression in Election. In contrast, in Crypto and Sports—where relationships are largely surface-level—CoT often introduces unnecessary noise, leading to drops in Accuracy. Overall, rationale generation enhances performance when reasoning complexity is high, but can be detrimental when simple textual cues suffice.

Ground-truth opinion graphs show clear higher-order structure. Although the benchmark labels pairwise correlations, these links form cohesive multi-event networks. As shown in Table 1, across all domains, 92–99% of events belong to a single connected component. Clustering coefficients are 12–29× higher than random (Politics: 0.088 vs. 0.003; Election: 0.257 vs. 0.012), revealing abundant triangular motifs. Louvain detection yields modularity of 0.50–0.77, well above random partitions. These results show that pairwise correlations naturally organize into structured, high-order opinion graphs, allowing pairwise evaluation to probe broader belief dynamics.

LLM-predicted graphs preserve key structural patterns. We then assess whether model-predicted graphs retain the structural properties of ground truth. As shown in Table 1, in *Election* and *Crypto*, connectivity and clustering closely match ground truth (<2% difference), with identical modularity in *Crypto* (0.578). Strength correlations (weighted degrees) exceed 0.95 across all domains. Transitivity, reflecting logical consistency, remains high (76–92%) and far above random baselines ($\approx 41\%$).

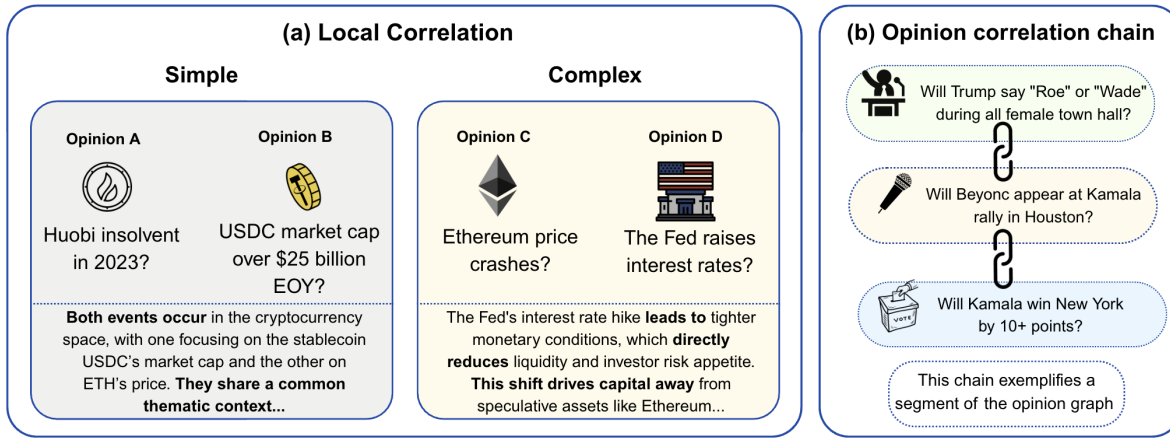


Figure 4: Case study for edges between social opinions and the path they form. (a) Pairwise relevance cases: GPT-4o+CoT explains both simple and complex social opinion pairs. (b) An example social opinion chain constructed from high-relevance event pairs (score > 0.6), with links inferred by GPT-4o using CoT reasoning.

Politics shows moderate degradation (83% vs. 93% GT connectivity), while Sports has lower connectivity (45%) but exceptionally high transitivity (98%), indicating locally consistent yet globally fragmented predictions. Overall, LLMs preserve network structure in semantically coherent domains and maintain local consistency even when global alignment weakens.

8 Case Study

Beyond statistical evaluation results on edge and graph prediction, we conduct microscopic case studies to examine how well LLM-based predictors reconstruct opinion graphs at two structural levels: *edges* and *paths*. This hierarchical perspective reveals how LLM-based rationale prediction can be used to make local predictions scale into global graph structure discovery. Additional examples are provided in Appendix §E.

Edge level: local correlations and reasoning rationales. Edges in the opinion graph can be supported by either simple or complex reasoning. Figure 4(a, left) shows a **simple** case, where two opinions share a clear topical overlap (e.g., both concern cryptocurrency but focus on different coins). The model's rationale is straightforward—it notes that they “share a common thematic context.” In contrast, Figure 4(a, right) presents a **complex** case, where the connection depends on multi-step temporal or causal reasoning. For example, a Federal Reserve interest rate hike can tighten monetary conditions and redirect capital away from speculative assets like Ethereum, linking two seemingly distant opinions. Together, these simple topical links and complex causal chains form the backbone of the

opinion graph structure.

Path level: chaining social opinions and the butterfly effect. Building on both simple and complex edges, Figure 4(b) shows how related opinions can form extended chains (paths in the opinion graph) through shared entities or causal dependencies. For example, a sequence linking Trump’s campaign statements to rally participation and ultimately to electoral outcomes illustrates how opinions evolve across interconnected contexts. Simple edges link central events to related ones, while complex edges propagate these connections across domains, creating reasoning paths that reflect the *butterfly effect*—where local signals spread through institutional or topical structures to shape broader expectations. These case studies demonstrate that LLMs can uncover such latent chains and generate coherent, evolving rationales that connect multiple social opinions, ultimately revealing the hidden structure underlying collective beliefs.

9 Discussion

To understand when and why LLMs succeed at uncovering social opinion structures, we focus on four key factors. We examine how performance varies across domains with different semantic structures (RQ1) and investigate the reasoning strategies models use to make predictions (RQ2). We then assess whether scaling and fine-tuning smaller models can improve efficiency without sacrificing accuracy (RQ3), and evaluate the role of knowledge recency in generalizing to unseen events (RQ4).

RQ1: What domain are LLMs good at?

LLMs perform well in semantically dense domains but struggle in sparse ones. As shown in Figure 3,

443
444
445
446
447
448
449
450

451
452
453
454
455
456
457
458
459
460

461
462
463
464
465
466
467
468
469
470
471
472
473
474
475
476

477
478
479
480
481
482
483
484
485
486
487
488
489
490
491
492
493
494
495
496

497
498
499
500
501
502
503
504
505
506
507
508
509
510

511
512
513
514
515
516
517
518
519
520
521
522
523
524
525
526
527
528
529
530
531
532
533
534
535
536
537
538
539
540
541
542
543
544
545
546
547
548
549
550
551
552
553
554
555
556
557
558
559
560
561

model performance varies by domain structure. In Crypto and Election, where events share entities, timelines, or institutions, models achieve stronger results. Even simple heuristics perform well due to the rich semantic context. In contrast, Sports events are often isolated and actor-specific, leading to the weakest performance. Political events fall in between, requiring both structural and contextual reasoning. These patterns suggest that LLMs are most effective in domains with coherent and recurring semantics.

RQ2: How do LLMs reason for prediction?

To better understand what types of relationships LLMs rely on when judging social opinion correlation, we analyze their CoT outputs and categorize the reasoning basis. As shown in Figure 5, only a small fraction of cases reflect explicit logical connections: approximately 8.7% in politics and less than 5.7% in sports. In contrast, a large proportion of predictions fall under *confounding* relationships (e.g., shared context or common background factors), accounting for 55% in politics and 32% in sports. These results suggest that LLMs do not primarily rely on formal logic or direct causality. Instead, they often identify perceived connections through narrative, intuition, or shared framing. This supports our interpretation that the LLM captures *relatedness* rather than *causal inference*.

RQ3: Does training on LLMs improve performance for edge prediction?

As shown in Figure 3, fine-tuning significantly boosts the performance of smaller models for opinion graph prediction. We fine-tuned Qwen1.5-4B on 500 social opinion pairs and evaluated it on the same test set. The fine-tuned model shows substantial gains over its zero-shot version and becomes competitive with much larger models, achieving performance comparable to Meta-Llama3-70B in certain domains. These results suggest that smaller, specialized models can serve as efficient and effective alternatives to large general-purpose LLMs.

RQ4: Does the knowledge cutoff matter?

We investigate whether LLMs rely on factual knowledge from pretraining or can generalize to unseen events. To this end, we compare model performance on event pairs occurring before and after the model’s knowledge cutoff. As shown in Figure 2, all evaluated models exhibit clear performance degradation on post-cutoff examples in the *election* domain, measured by percentage change in MSE. For instance, GPT-4o shows a substantial

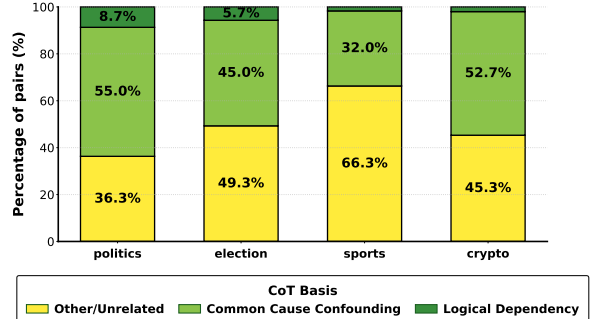


Figure 5: **Distribution of reasoning types across domains.** Each edge was labeled based on the explanation produced by the model. A majority of predictions are based on shared context (*confounding*) or loose narrative links (*CoT basis*), while only a small portion exhibit explicit logical or causal reasoning. This suggests the model is primarily identifying correlations rather than inferring direct causal links.

Model	Before↓	After↓	Δ (%)
Heuristic (Time-OL)	0.0639	—	—
LLaMA	0.0556	0.0656	+18.0
DeepSeek v3	0.0318	0.0348	+9.4
GPT-4o	0.0167	0.0252	+50.9

Table 2: **Results on temporal generalization.** We report MSE before/after the knowledge cutoff (Election). All models exhibit worse MSE performance on post-cutoff event pairs, highlighting challenges in temporal generalization. GPT-4o shows the highest increase. Time-OL represents time-overlapping.

drop of over 50%, while DeepSeek-v3 and LLaMA-3 also experience notable declines. These results suggest that while LLMs may generalize to unseen patterns to some extent, their ability to capture social opinion correlation often depends on up-to-date world knowledge learned during pretraining.

10 Conclusion

In summary, social opinions form richly structured networks and make graph-based representations a natural framework for understanding collective belief dynamics. By leveraging high-quality opinion graphs and applying LLMs to edge prediction tasks, we show that LLMs not only excel at predicting pairwise relations but also recover higher-order structural patterns that closely mirror ground-truth networks. These findings demonstrate that LLMs implicitly capture the latent organization of social opinions, enabling scalable analysis of emerging belief dynamics. Looking ahead, our framework can motivate future work for better studies on opinion dynamics and social simulation.

583 Limitations

584 **Heuristic-score-based ground truth** Our
585 ground-truth labels are derived from a weighted
586 heuristic score $S(A, B)$ that combines temporal
587 synchrony, textual similarity and time alignment
588 (see Section §4.2). Although this method improves
589 over pure correlation-based approaches (e.g.
590 Kendall's τ), it can still assign high scores to
591 spurious pairs, for example events with spikes
592 in coincident volatility or shared metadata but
593 without substantive connection. Such false
594 positives can penalize models that correctly reject
595 these superficial links, limiting the fidelity of the
596 supervision signal.

597 **Platform and domain bias.** Polymarket does not
598 list every real-world event - in many domains, the
599 coverage is patchy.

600 **Pairwise relation assumption.** Our framework
601 estimates the strength of social opinion correlations
602 using pairwise relationships between events.
603 While this design enables interpretable and scalable
604 analysis, it does not explicitly capture higher-order
605 dependencies among multiple events. Future work
606 could explore multi-event or graph-based inference
607 methods to model collective reasoning patterns that
608 go beyond pairwise interactions.

609 **Temporal overlap assumption.** Our approach
610 focuses on social opinion pairs with overlapping
611 active periods to ensure that the measured time-
612 series correlations capture dynamic co-movement
613 as traders respond to new information. While this
614 design helps reduce noise in estimating relevance,
615 it also limits the benchmark's ability to evaluate
616 delayed or indirect causal links that might manifest
617 outside of these overlapping windows. Future work
618 could explore more advanced temporal modeling
619 strategies, such as lag-aware correlation measures
620 or causal inference techniques to better capture
621 these complex, cross-temporal relationships.

622 Ethical Statement

623 This work analyzes public event data from Poly-
624 market, a prediction market platform that provides
625 open-access market-level data without any user-
626 identifiable information. We do not collect or pro-
627 cess individual-level data, and all analysis is con-
628 ducted at the event level. Thus, privacy concerns
629 are minimal.

630 Our evaluation framework involves using large
631 language models (LLMs) to assess the relevance be-

632 tween social events. These models, while powerful,
633 may exhibit unintended biases, particularly in po-
634 litically sensitive or socially charged domains. We
635 caution against using these models as authoritative
636 predictors or decision-making tools in high-stakes
637 environments.

638 Additionally, while our work aims to understand
639 event relationships, it does not attempt to fore-
640 cast outcomes or provide trading recommendations.
641 The models are evaluated solely on their reason-
642 ing and ranking capability and should not be inter-
643 preted as reliable financial or political forecasting
644 instruments.

645 Finally, while our method is training-free, the
646 evaluation dataset itself may reflect biases from
647 Polymarket's coverage, which is shaped by com-
648 munity interest and market dynamics. As a result,
649 certain domains, such as Sports or Politics, may
650 be overrepresented, potentially influencing model
651 predictions or evaluation trends. We encourage fu-
652 ture work to broaden coverage to include a more
653 balanced set of social domains.

654 References

2024. The llama 3 herd of models. *Preprint*,
655 arXiv:2407.21783.

2024. Qwen2 technical report. *Preprint*,
657 arXiv:2407.10671.

2025a. Deepseek-r1: Incentivizing reasoning capa-
659 bility in llms via reinforcement learning. *Preprint*,
660 arXiv:2501.12948.

2025b. Deepseek-v3 technical report. *Preprint*,
662 arXiv:2412.19437.

Anonymous. 2025. Title omitted for double-blind re-
664 view. Under review.

666 Tristan J. B. Cann, Ben Dennes, Travis Coan, Saffron
667 O'Neill, and Hywel T. P. Williams. 2023. Using
668 semantic similarity and text embedding to measure
669 the social media echo of strategic communications.
670 *Preprint*, arXiv:2303.16694.

671 Mario Cataldi, Luigi Di Caro, and Claudio Schifanella.
672 2010. Emerging topic detection on twitter based on
673 temporal and social terms evaluation. In *Proceedings*
674 of the Tenth International Workshop on Multimedia
675 Data Mining, MDMKDD '10, New York, NY, USA.
676 Association for Computing Machinery.

677 Minje Choi, Jiaxin Pei, Sagar Kumar, Chang Shu, and
678 David Jurgens. 2023. Do LLMs understand social
679 knowledge? evaluating the sociability of large lan-
680 guage models with SocKET benchmark. In *Proceed-
681 ings of the 2023 Conference on Empirical Methods in*

682	<i>Natural Language Processing</i> , pages 11370–11403, Singapore. Association for Computational Linguistics.	737
683		738
684		739
685		740
686		
687		
688		
689		
690		
691		
692		
693		
694		
695		
696		
697		
698		
699		
700		
701		
702		
703		
704		
705		
706		
707		
708		
709		
710		
711		
712		
713		
714		
715		
716		
717		
718		
719		
720		
721		
722		
723		
724		
725		
726		
727		
728		
729		
730		
731		
732		
733		
734		
735		
736		
737	Taiwo Kolajo, Olawande Daramola, and Ayodele A Adebiyi. 2022. Real-time event detection in social media streams through semantic analysis of noisy terms. <i>Journal of Big Data</i> , 9(1):90.	740
738		
739		
740		
741	Jean Lee, Nicholas Stevens, and Soyeon Caren Han. 2025. Large language models in finance (finllms). <i>Neural Computing and Applications</i> .	743
742		
743		
744	Lincan Li, Jiaqi Li, Catherine Chen, Fred Gui, Hongjia Yang, Chenxiao Yu, Zhengguang Wang, Jianing Cai, Junlong Aaron Zhou, Bolin Shen, Alex Qian, Weixin Chen, Zhongkai Xue, Lichao Sun, Lifang He, Hanjie Chen, Kaize Ding, Zijian Du, Fangzhou Mu, and 28 others. 2024. Political-llm: Large language models in political science. <i>Preprint</i> , arXiv:2412.06864.	750
745		
746		
747		
748		
749		
750		
751	Gosse Minnema, Huiyuan Lai, Benedetta Muscato, and Malvina Nissim. 2023. Responsibility perspective transfer for Italian femicide news. In <i>Findings of the Association for Computational Linguistics: ACL 2023</i> , pages 7907–7918, Toronto, Canada. Association for Computational Linguistics.	756
752		
753		
754		
755		
756		
757	Qiang Ning, Hao Wu, and Dan Roth. 2018. A multi-axis annotation scheme for event temporal relations. In <i>Proceedings of the 56th Annual Meeting of the Association for Computational Linguistics (Volume 1: Long Papers)</i> , pages 1318–1328, Melbourne, Australia. Association for Computational Linguistics.	762
758		
759		
760		
761		
762		
763	Hao Peng, Jianxin Li, Yangqiu Song, Renyu Yang, Rajiv Ranjan, Philip S. Yu, and Lifang He. 2021. Streaming social event detection and evolution discovery in heterogeneous information networks. <i>Preprint</i> , arXiv:2104.00853.	767
764		
765		
766		
767		
768	Kristina Radivojevic, Nicholas Clark, and Paul Brenner. 2024. Llms among us: Generative ai participating in digital discourse. In <i>Proceedings of the AAAI Symposium Series</i> , volume 3, pages 209–218.	771
769		
770		
771		
772	Abhinav Sukumar Rao, Akhila Yerukola, Vishwa Shah, Katharina Reinecke, and Maarten Sap. 2025. NormAd: A framework for measuring the cultural adaptability of large language models. In <i>Proceedings of the 2025 Conference of the Nations of the Americas Chapter of the Association for Computational Linguistics: Human Language Technologies (Volume 1: Long Papers)</i> , pages 2373–2403, Albuquerque, New Mexico. Association for Computational Linguistics.	780
773		
774		
775		
776		
777		
778		
779		
780		
781	Qwen Team. 2024. Introducing qwen1.5.	781
782	Qwen Team and 1 others. 2024. Qwen2 technical report. <i>arXiv preprint arXiv:2407.10671</i> , 2:3.	783
783		
784	Hugo Touvron, Thibaut Lavril, Gautier Izacard, Xavier Martinet, Marie-Anne Lachaux, Timothée Lacroix, Baptiste Rozière, Naman Goyal, Eric Hambro, Faisal Azhar, and 1 others. 2023. Llama: Open and efficient foundation language models. <i>arXiv preprint arXiv:2302.13971</i> .	789
785		
786		
787		
788		
789		

790 Haoyu Wang, Hongming Zhang, Kaijiang Song, Dong
791 Yu, and Dan Roth. 2024. **Event semantic classifi-**
792 **cation in context**. In *Findings of the Association*
793 *for Computational Linguistics: EACL 2024*, pages
794 1395–1407, St. Julian’s, Malta. Association for Com-
795 putational Linguistics.

796 Jason Wei, Xuezhi Wang, Dale Schuurmans, Maarten
797 Bosma, Fei Xia, Ed Chi, Quoc V Le, Denny Zhou,
798 and 1 others. 2022. Chain-of-thought prompting elicit-
799 its reasoning in large language models. *Advances*
800 *in neural information processing systems*, 35:24824–
801 24837.

802 Aaron Wheeler and Jeffrey D. Varner. 2024. **Mar-**
803 **ketgpt: Developing a pre-trained transformer (gpt)**
804 **for modeling financial time series**. *Preprint*,
805 arXiv:2411.16585.

806 Yuanjian Xu, Anxian Liu, Jianing Hao, Zhenzhuo Li,
807 Shichang Meng, and Guang Zhang. 2024. **Plutus:**
808 **A well pre-trained large unified transformer can**
809 **unveil financial time series regularities**. *Preprint*,
810 arXiv:2408.10111.

811 Ye Yuan, Kexin Tang, Jianhao Shen, Ming Zhang, and
812 Chenguang Wang. 2024. **Measuring social norms of**
813 **large language models**. In *Findings of the Associa-*
814 *tion for Computational Linguistics: NAACL 2024*,
815 pages 650–699, Mexico City, Mexico. Association
816 for Computational Linguistics.

817 Yucheng Zhou, Xiubo Geng, Tao Shen, Guodong Long,
818 and Dixin Jiang. 2021. **Eventbert: A pre-trained**
819 **model for event correlation reasoning**. *Preprint*,
820 arXiv:2110.06533.

821 Xiaojin Zhu, Zoubin Ghahramani, and John Lafferty.
822 2003. Semi-supervised learning using gaussian fields
823 and harmonic functions. *ICML’03*, page 912–919.
824 AAAI Press.

825 A Artifact Details

826 A.1 Artifact Information

827 This artifact contains all components required to
828 reproduce the results in our study of social opinion
829 correlation reasoning in large language models
830 (LLMs). It includes:

- 831 • **Code:** A complete implementation of the pair-
832 wise social opinion correlation scoring pipeline,
833 including preprocessing, model inference (with
834 and without CoT prompting), and evaluation
835 metrics.
- 836 • **Data:**
 - 837 – Manually annotated development and test
838 sets across four domains: Politics, Election,
839 Cryptocurrency, and Sports.
 - 840 – Rubric definitions used to guide annotation.
 - 841 – Annotation metadata and inter-annotator
842 agreement statistics.
- 843 • **Models:** Inference scripts for querying multiple
844 foundation models via standard APIs. Specifically,
845 GPT-4o and GPT-o3-mini were accessed
846 through the official OpenAI API, while Meta-
847 Llama-3, DeepSeek-V3, and Qwen2 series were
848 accessed via the Together.ai inference platform.
849 All calls are wrapped with reproducible config-
850 urations, and API versions are specified to en-
851 sure consistent results across runs. For models
852 supporting CoT prompting, the corresponding
853 CoT-enabled variants are also included.
- 854 • **Evaluation:** Scripts to compute both regression
855 and classification metrics, including MSE, MAE,
856 Accuracy, Macro-F1, QWK. Also included are
857 scripts to produce the figures and tables in the
858 main paper and appendix.
- 859 • **Case Study Tools:** Utilities for constructing so-
860 cial opinion chains, visualizing social opinion
861 graphs, and analyzing CoT rationales.

862 The artifact is designed for easy replication and
863 modification. Each script is documented with usage
864 instructions, input formats, and expected outputs.
865 Running the default configuration will reproduce
866 all key results from the paper. At the time of sub-
867 mission, these materials are under preparation for
868 release. We will make the code and data available
869 upon publication.

870 A.2 Artifact License

871 All components of our artifact are intended for
872 research use and will be released under open-source
873 or permissive licenses upon publication.

- 874 • **Codebase:** The full codebase, including prepro-
875 cessing, inference, and evaluation scripts, will be
876 released under the MIT License.

- 877 • **Annotated Data:** The manually labeled develop-
878 ment and test sets, along with rubric definitions
879 and annotation metadata, are original contribu-
880 tions of this work. These datasets will be released
881 under the CC BY 4.0 License, permitting reuse
882 with attribution for research and non-commercial
883 purposes.

- 884 – **Codebase:** The full codebase, including pre-
885 processing, inference, and evaluation scripts,
886 will be released under the MIT License.

- 887 – **Annotated Data:** The manually labeled devel-
888 opment and test sets, along with rubric defi-
889 nitions and annotation metadata, are original
890 contributions of this work. These datasets will
891 be released under the CC BY 4.0 License, per-
892 mitting reuse with attribution for research and
893 non-commercial purposes.

- 894 – **Model Usage:** Our study relies on querying
895 several pretrained language models. We use
896 **GPT-4o** and **GPT-o3-mini** via the OpenAI
897 API,³ which are proprietary models licensed
898 by OpenAI. We also evaluate open-weight
899 models including **Meta-Llama-3 70B** (gra,
900 2024), **DeepSeek-V3** (dee, 2025b), **DeepSeek-**
901 **R1** (dee, 2025a), and **Qwen2** (yan, 2024),
902 accessed through the Together.ai inference plat-
903 form, all released under Apache 2.0 or simi-
904 lar permissive licenses. In addition, we fine-
905 tune **Qwen1.5-4B** (Team, 2024) (LoRA vari-
906 ant) using the Hugging Face Transformers li-
907 brary,⁴ which is an open-weight model under
908 the Apache 2.0 License. The fine-tuning was
909 performed on a single NVIDIA A100 GPU for
910 approximately 10 minutes, with no large-scale
911 computational resources required. For com-
912 parison, we include a **cross-encoder baseline**
913 using **nli-deberta-v3-base**⁵ from Hugging
914 Face, licensed under the MIT License.

915 We respect all license terms associated with the
916 use of these third-party models and APIs. No
917 model weights are redistributed. All data and code
918 will be clearly marked with their respective licenses
919 in the released repository.

³<https://platform.openai.com/docs/models/gpt-4o>

⁴<https://huggingface.co/Qwen/Qwen1.5-4B>

⁵<https://huggingface.co/cross-encoder/nli-deberta-v3-base>

920 A.3 Data Usage

921 Our dataset includes events across four domains:
 922 Politics, Election, Cryptocurrency, and Sports. We
 923 use a subset of Polymarket data curated by prior
 924 work currently under review (Anonymous, 2025).
 925 The final dataset will be released under the MIT
 926 License for academic use.

- 927 • **Source and Licensing:**

- 928 • **Use Consistency:** Our data usage is consistent
 929 with the intended purpose of the source materials,
 930 which were either licensed for research or cre-
 931 ated explicitly for this project. No repurposing
 932 beyond research evaluation has been conducted.

- 933 • **Human Annotation:** Each social opinion corre-
 934 lation pair in the development and test sets was
 935 labeled by multiple annotators using a rubric-
 936 based scale. Inter-annotator agreement scores are
 937 included in the Appendix §I to reflect labeling
 938 quality.

- 939 • **Privacy and Safety:** The dataset does not con-
 940 tain any personally identifiable information (PII),
 941 user metadata, or social media handles. All
 942 text has been reviewed to exclude offensive con-
 943 tent, and no inference was made regarding demo-
 944 graphic or protected attributes.

- 945 • **Intended Use:** The dataset is intended exclu-
 946 sively for research on social reasoning, social
 947 opinion dynamics, and LLM evaluation. It is
 948 not suitable for deployment in user-facing appli-
 949 cations or downstream tasks involving sensitive
 950 decision-making.

951 A.4 Data Statistics

952 Our benchmark covers four domains: Politics, Elec-
 953 tion, Cryptocurrency, and Sports.

954 The final benchmark includes:

- 955 • **Total event pairs:** 8,839
- 956 • **Label format:** Each pair is assigned a con-
 957 tinuous social opinion correlation score in the
 958 range $[0, 1]$, reflecting graded relatedness. For
 959 classification-based analyses, scores are mapped
 960 to a 5-point ordinal scale (from strongly unrelated
 961 to strongly related) using predefined thresholds.
- 962 • **Label source:** The majority of labels were de-
 963 rived programmatically via rubric-based scoring;
 964 a small subset was verified by human annotators
 965 for calibration and quality assurance.
- 966 • **Agreement check:** For the verified subset, each
 967 pair was annotated by 3 annotators. The average
 968 inter-annotator correlation exceeds 0.78, indicat-
 969 ing strong agreement on the ordinal scale used

970 for verification.

971 B Computational Resources.

972 The only locally fine-tuned model was **Qwen1.5-973 4B (LoRA)**, trained on a single NVIDIA A100
 974 GPU (80GB) for approximately 10 minutes, corre-
 975 sponding to a total compute budget of ~ 0.17 GPU-
 976 hours. The LoRA adapters introduce fewer than 1%
 977 of the base model’s parameters. All other models
 978 were accessed via the OpenAI and Together.ai in-
 979 ference APIs, requiring no additional training. All
 980 runs were executed deterministically with fixed ran-
 981 dom seeds and single-threaded decoding to ensure
 982 reproducibility.

983 C Dataset Construction Details

984 C.1 Volatility filter details

985 We include the volatility filter here. Let $r_t =$
 986 $\text{logit}(p_t) - \text{logit}(p_{t-1})$ be logit return, *i.e.*, day-
 987 to-day changes in log-odds. Denote by $\sigma_t^{(w)}$ the
 988 rolling standard deviation of $\{r_\tau\}_{\tau=t-w+1}^t$ over a
 989 window of w days. Let γ be the volatility threshold
 990 and α be the required proportion. We retain a base
 991 market only if

$$992 \frac{1}{T-w+1} \sum_{t=w}^T \mathbf{1}[\sigma_t^{(w)} \geq \gamma] \geq \alpha, \quad (4)$$

993 *i.e.*, at least α fraction of the windows have the
 994 standard deviation of the daily logit returns above
 995 γ .

996 C.2 Edge construction feature details

997 **Feature1: Change-point synchrony.** We iden-
 998 tify time points where an event’s social opinion
 999 trajectory exhibits statistically significant shifts by
 1000 applying z-score thresholding to the price deltas
 1001 in its time series. For each event, we extract a set
 1002 of such change points. The synchrony score then
 1003 measures the fraction of change points in event A
 1004 that align within a short temporal window δ of any
 1005 change point in event B . This captures the intuition
 1006 that jointly fluctuating social opinions are likely to
 1007 be correlated:

$$1008 s_1(A, B) = \frac{1}{|T_A|} \sum_{t \in T_A} \mathbb{1}[\exists t' \in T_B, |t - t'| < \delta]. \quad (5)$$

1009 **Feature2: Tag Jaccard similarity.** To estimate
 1010 topical overlap, we use the Jaccard index over tag

1011 sets from Polymarket metadata. Each event includes tags that describe its domain or subject matter. A high Jaccard score indicates that two events
 1012 are framed under similar categories or themes, which may reflect a shared discourse context:
 1013
 1014
 1015

$$s_2(A, B) = \frac{|\mathcal{K}_A \cap \mathcal{K}_B|}{|\mathcal{K}_A \cup \mathcal{K}_B|}. \quad (6)$$

1017 **Feature3: Minimum time gap.** We compute the
 1018 minimum absolute time difference between any
 1019 change point in event A and any in event B . This
 1020 measures how closely social opinion shifts in the
 1021 two events occur in time. We convert this to a soft
 1022 similarity score using a monotonic inverse transforma-
 1023 tion:

$$s_3(A, B) = \frac{1}{1 + \min_{t \in T_A, t' \in T_B} \frac{|t - t'|}{\tau}}. \quad (7)$$

1024 **Feature4: Textual similarity.** We embed the text
 1025 descriptions of events using sentence-transformer
 1026 models and compute cosine similarity between the
 1027 resulting embeddings. This feature captures semantic
 1028 proximity at the lexical and conceptual level,
 1029 and complements the tag-based feature with more
 1030 nuanced language modeling:
 1031

$$s_4(A, B) = 1 - \cos(\mathbf{e}_A, \mathbf{e}_B). \quad (8)$$

1032 **Overall.** The four feature scores are linearly com-
 1033 bined into a single heuristic correlation score. The
 1034 weights are optimized on a development set to
 1035 best match human relevance judgments. We dis-
 1036 cretize $S(A, B)$ into five relevance classes: *very*
 1037 *weak* (0.0–0.2), *weak* (0.2–0.4), *medium* (0.4–0.6),
 1038 *strong* (0.6–0.8), and *very strong* (0.8–1.0). These
 1039 bucketed labels serve as groundtruth in evaluation:
 1040

$$S(A, B) = \sum_{i=1}^4 w_i \cdot s_i(A, B) \quad (9)$$

1041 where w_i is tuned to make the prediction highly
 1042 aligned with a small set of human annotation
 1043 results. The final normalized weights are:
 1044 $w_{\text{sync}}=0.2688$, $w_{\text{jacc}}=0.3652$, $w_{\text{time}}=0.1228$, and
 1045 $w_{\text{text}}=0.2435$.
 1046

D LLM Prompt

1047 The prompt of the zero shot and CoT version are
 1048 in Table 3
 1049

E Case Study Examples

E.1 Simple

1050 These pairs are topically similar but lack direct
 1051 causal or temporal connection.
 1052

1053 **Example 1 Event 1:** USDC market cap over \$25
 1054 billion EOY?
 1055

1056 **Event 2:** Will ETH hit \$2,000 by EOY?
 1057

1058 **Ground Truth:** 0.4–0.6
 1059

1060 **GPT-o3-mini (CoT):** 0.2–0.4
 1061

1062 **GPT-o3-mini (No CoT):** 0.4–0.6
 1063

1064 **CoT:** "Both events occur in the cryptocurrency
 1065 space, with one focusing on the stablecoin USDC's
 1066 market cap and the other on ETH's price. They
 1067 share a common thematic context but are mea-
 1068 suring distinct characteristics of the crypto mar-
 1069 ket with minimal direct causal influence between
 1070 them."
 1071

1072 **Example 2 Event 1:** Will ETH hit \$2,000 by
 1073 EOY?
 1074

1075 **Event 2:** Huobi insolvent in 2023?
 1076

1077 **Ground Truth:** 0.4–0.6
 1078

1079 **GPT-o3-mini (CoT):** 0.2–0.4
 1080

1081 **GPT-o3-mini (No CoT):** 0.4–0.6
 1082

1083 **CoT:** "Both events relate to the cryptocurrency in-
 1084 dustry. However, while ETH reaching a certain
 1085 price is a market performance event, Huobi's insol-
 1086 vency is a corporate financial event. Their connec-
 1087 tion is thematic but not directly causal or tempo-
 1088 rally linked."
 1089

E.2 Complex

1090 These examples involve shared actors, institutional
 1091 decisions, or policy-level connections.
 1092

1093 **Example 3 Event 1:** Will SEC delay Bitcoin
 1094 ETF decision?
 1095

1096 **Event 2:** Ethereum spot ETF approved by Mar 31?
 1097

1098 **Ground Truth:** 0.6–0.8
 1099

1100 **GPT-o3-mini (CoT):** 0.6–0.8
 1101

1102 **GPT-o3-mini (No CoT):** 0.4–0.6
 1103

1104 **CoT:** "Both events involve SEC decisions regard-
 1105 ing cryptocurrency ETFs. They are thematically
 1106 linked, as they both pertain to regulatory actions on
 1107 crypto investments and have overlapping timelines,
 1108 despite focusing on different digital assets (Bitcoin
 1109 and Ethereum)."
 1110

1111 **Example 4 Event 1:** Will Haley beat DeSantis
 1112 in Iowa?
 1113

1114 **Event 2:** Will Kristi Noem win the U.S. 2024 Re-
 1115 publican VP nomination?
 1116

Original Prompt	CoT Prompt
<p>You are an expert in interpreting and reasoning about real-world events, such as those found on prediction markets.</p> <p>Your task is to read two events and classify how related they are using <i>exactly one</i> of the label keys below. Base your judgement on any causal, temporal, or thematic relationship that may exist.</p> <p>Return only a valid JSON object in the form: <code>{"label": "0.4-0.6"}</code>. Do <i>not</i> include explanations, formatting, or any additional text.</p> <p>Labels (choose one key only):</p> <p><code>"0.0-0.2"</code> → Unrelated — No real connection in topic, time, or influence.</p> <p><code>"0.2-0.4"</code> → Weakly Related — Small thematic overlap, but no causal or temporal influence.</p> <p><code>"0.4-0.6"</code> → Moderately Related — Events share context or actors but remain largely independent.</p> <p><code>"0.6-0.8"</code> → Strongly Related — One event influences or is likely affected by the other.</p> <p><code>"0.8-1.0"</code> → Highly Related — One event is clearly a consequence, cause, or restatement of the other.</p> <p>Event 1 <code>{e1_title}</code> <code>{e1_desc}</code></p> <p>Event 2 <code>{e2_title}</code> <code>{e2_desc}</code></p> <p>Strictly respond with a JSON object like: <code>{"label": "0.6-0.8"}</code></p>	<p>You are an expert in interpreting and reasoning about real-world events, such as those found on prediction markets.</p> <p>Your task is to read two events and classify how related they are using <i>exactly one</i> of the label keys below. Base your judgement on any causal, temporal, or thematic relationship that may exist.</p> <p>First, in <i>a few concise sentences</i>, explain any causal, temporal, or thematic links you see.</p> <p>Then, on a new line, output <i>ONLY</i> one valid JSON object like: <code>{"label": "0.4-0.6"}</code>. Do <i>not</i> include any additional text.</p> <p>Labels (choose one key only):</p> <p><code>"0.0-0.2"</code> → Unrelated — No real connection in topic, time, or influence.</p> <p><code>"0.2-0.4"</code> → Weakly Related — Small thematic overlap, but no causal or temporal influence.</p> <p><code>"0.4-0.6"</code> → Moderately Related — Events share context or actors but remain largely independent.</p> <p><code>"0.6-0.8"</code> → Strongly Related — One event influences or is likely affected by the other.</p> <p><code>"0.8-1.0"</code> → Highly Related — One event is clearly a consequence, cause, or restatement of the other.</p> <p>Event 1 <code>{e1_title}</code> <code>{e1_desc}</code></p> <p>Event 2 <code>{e2_title}</code> <code>{e2_desc}</code></p> <p>Give your concise reasoning, <i>then</i> output the JSON object on the next line.</p>

Table 3: Comparison of Original vs. CoT prompt templates

1098 **Ground Truth:** 0.2–0.4
1099 **GPT-o3-mini (CoT):** 0.2–0.4
1100 **GPT-o3-mini (No CoT):** 0.4–0.6
1101 **CoT:** "Both events occur within the context of U.S.
1102 Republican political dynamics in the 2024 election
1103 cycle, sharing a general theme of intra-party com-
1104 petition. However, they concern distinct contests
1105 with different candidates and positions, and there
1106 is no direct causal or temporal link between them."
1107 We include the full benchmark results across all
1108 domains and metrics in Tables 4–7.

1109 **F Full Benchmark Results**

1110 We include the full benchmark results across all
1111 domains and metrics in Tables 4–7.

1112 **G Use Of AI Assistants**

1113 We did use ChatGPT as the writing assistant to
1114 help us write part of the paper. Additionally, we
1115 utilize the power of CodePilot to help us code faster.
1116 However, all the AI-generated writing and coding
1117 components assisted by AI are manually checked
1118 and modified. There is no full AI-generated content
1119 in the paper.

Method	MSE	MAE	Accuracy	Macro-F1	QWK
random	0.1459	0.3130	0.1977	0.1377	0.0071
heuristic (vol. max→min)	0.0411	0.1674	0.2860	0.0910	-0.0040
heuristic (vol. sim.)	0.1113	0.3003	0.0691	0.0414	0.0089
heuristic (time overlap)	0.0459	0.1687	0.3437	0.1913	0.1121
GPT-4o	0.0234	0.1258	0.4317	0.2978	0.4094
GPT-4o + CoT	0.0250	0.1214	0.5116	0.2621	0.2843
GPT-o3-mini	0.0253	0.1322	0.3973	0.2722	0.3415
GPT-o3-mini + CoT	0.0188	0.1147	0.4561	0.2411	0.3238
Meta-Llama3-70B	0.0377	0.1532	0.3847	0.2543	0.4084
Meta-Llama3-70B + CoT	0.0327	0.1518	0.3400	0.2593	0.3887
DeepSeek-V3	0.0250	0.1291	0.4383	0.3100	0.4105
DeepSeek-V3 + CoT	0.0236	0.1286	0.4006	0.2752	0.3697
DeepSeek-R1	0.0830	0.2600	0.0940	0.0807	0.0786
DeepSeek-R1 + CoT	0.0512	0.1996	0.1959	0.1585	0.1162
Qwen2-72B	0.0309	0.1426	0.3800	0.2292	0.3526
Qwen2-72B + CoT	0.0338	0.1534	0.3200	0.2285	0.2749
cross-encoder (nli-deberta-v3-base)	0.0519	0.1812	0.2797	0.0969	0.1076
Qwen1.5-4B (zero-shot)	0.0839	0.2109	0.2960	0.1038	0.0311
Qwen1.5-4B (fine-tuned, LoRA)	0.0351	0.1300	0.4362	0.1813	0.1752

Table 4: **Performance on Politics domain.** Evaluation across selected metrics.

Method	MSE	MAE	Accuracy	Macro-F1	QWK
random	0.1330	0.3000	0.2019	0.1541	0.0125
heuristic (vol. max→min)	0.0878	0.2447	0.1430	0.0560	-0.0140
heuristic (vol. sim.)	0.0945	0.2645	0.1403	0.0864	0.0398
heuristic (time overlap)	0.0779	0.2274	0.2179	0.1344	0.1427
tag overlap*	0.0152	0.1014	0.5471	0.5691	0.6999
GPT-4o	0.0252	0.1265	0.4683	0.3584	0.5227
GPT-4o + CoT	0.0256	0.1274	0.4433	0.2687	0.4447
GPT-o3-mini	0.0412	0.1549	0.4284	0.3360	0.4645
GPT-o3-mini + CoT	0.0543	0.1638	0.4632	0.3531	0.5011
Meta-Llama3-70B	0.0416	0.1640	0.3828	0.3349	0.5004
Meta-Llama3-70B + CoT	0.0364	0.1612	0.3303	0.3278	0.4733
DeepSeek-V3	0.0242	0.1230	0.4974	0.3428	0.5187
DeepSeek-V3 + CoT	0.0289	0.1402	0.3963	0.3244	0.4886
DeepSeek-R1	0.0441	0.1833	0.2206	0.1137	0.1267
DeepSeek-R1 + CoT	0.0352	0.1698	0.2320	0.1420	0.0713
Qwen2-72B	0.0336	0.1488	0.4067	0.3069	0.4024
Qwen2-72B + CoT	0.0387	0.1683	0.2867	0.2385	0.3550
cross-encoder (nli-deberta-v3-base)	0.0888	0.2483	0.1466	0.0967	0.1491
Qwen1.5-4B (zero-shot)	0.1203	0.2693	0.2433	0.1691	0.1800
Qwen1.5-4B (fine-tuned, LoRA)	0.0760	0.1942	0.3592	0.3326	0.4519

Table 5: **Performance on Cryptocurrency domain.** Evaluation across selected metrics.

*Note: the "tag overlap" method was used as a feature in the creation of the ground-truth labels (see Section 5.2 and is therefore not a benchmark baseline.

Method	MSE	MAE	Accuracy	Macro-F1	QWK
random	0.1423	0.3093	0.2016	0.1759	0.0099
heuristic (vol. max→min)	0.1612	0.3197	0.1090	0.0490	-0.0030
heuristic (vol. sim.)	0.0885	0.2531	0.1780	0.1289	0.0941
heuristic (time overlap)	0.0877	0.2383	0.2157	0.2058	0.4190
tag overlap*	0.0229	0.1298	0.4407	0.4982	0.7932
GPT-4o	0.1042	0.2558	0.1746	0.1431	0.2418
GPT-4o + CoT	0.0744	0.2209	0.2267	0.1890	0.3678
GPT-o3-mini	0.0931	0.2305	0.2840	0.2383	0.4805
GPT-o3-mini + CoT	0.1199	0.2654	0.2182	0.1922	0.3620
Meta-Llama3-70B	0.0772	0.2312	0.1813	0.1790	0.4399
Meta-Llama3-70B + CoT	0.0838	0.2404	0.1629	0.1523	0.3916
DeepSeek-V3	0.0884	0.2432	0.1678	0.1558	0.3438
DeepSeek-V3 + CoT	0.0909	0.2480	0.1500	0.1305	0.3026
DeepSeek-R1	0.0258	0.1307	0.4409	0.4599	0.3327
DeepSeek-R1 + CoT	0.0442	0.1625	0.3972	0.2620	0.3454
Qwen2-72B	0.0983	0.2422	0.2000	0.1751	0.2478
Qwen2-72B + CoT	0.1006	0.2476	0.1933	0.1625	0.2499
cross-encoder (nli-deberta-v3-base)	0.1779	0.3432	0.0916	0.0496	-0.0360
Qwen1.5-4B (zero-shot)	0.1463	0.3033	0.2000	0.1290	0.0018
Qwen1.5-4B (test metrics)	0.1286	0.2788	0.2850	0.1834	0.1468

Table 6: **Performance on Sports domain.** Evaluation across selected metrics.

*Note: the "tag overlap" method was used as a feature in the creation of the ground-truth labels (see Section 5.2 and is therefore not a benchmark baseline.

Method	MSE	MAE	Accuracy	Macro-F1	QWK
random	0.1268	0.2914	0.2058	0.1558	0.0077
heuristic (vol. max→min)	0.0719	0.2227	0.1940	0.0870	-0.0200
heuristic (vol. sim.)	0.0850	0.2504	0.1610	0.0835	0.0181
heuristic (time overlap)	0.0639	0.2063	0.2570	0.1906	0.1380
tag overlap*	0.0175	0.1121	0.4721	0.5775	0.6283
GPT-4o	0.0219	0.1112	0.5575	0.2940	0.3522
GPT-4o + CoT	0.0346	0.1489	0.4033	0.3100	0.4149
GPT-o3-mini	0.0278	0.1344	0.4548	0.2088	0.2752
GPT-o3-mini + CoT	0.0231	0.1187	0.5451	0.2496	0.4183
Meta-Llama3-70B	0.0596	0.1970	0.3103	0.2468	0.3598
Meta-Llama3-70B + CoT	0.0470	0.1834	0.2660	0.2118	0.3397
DeepSeek-V3	0.0330	0.1456	0.4132	0.2953	0.4087
DeepSeek-V3 + CoT	0.0312	0.1450	0.3836	0.2930	0.4197
DeepSeek-R1	0.0441	0.1833	0.2206	0.1137	0.1267
DeepSeek-R1 + CoT	0.0220	0.1192	0.4636	0.1893	0.1715
Qwen2-72B	0.0430	0.1696	0.3233	0.2345	0.4127
Qwen2-72B + CoT	0.0383	0.1639	0.3200	0.2737	0.4104
cross-encoder (nli-deberta-v3-base)	0.0972	0.2604	0.1436	0.0688	0.1117
Qwen1.5-4B (zero-shot)	0.2099	0.3650	0.2217	0.1162	0.0458
Qwen1.5-4B (fine-tuned, LoRA)	0.0681	0.2017	0.3058	0.2401	0.3873

Table 7: **Performance on Election domain.** Evaluation across selected metrics.

*Note: the "tag overlap" method was used as a feature in the creation of the ground-truth labels (see Section 5.2 and is therefore not a benchmark baseline.

Table 8: **Annotation scale with definitions and representative examples.** Each bin corresponds to a level of relevance used in rating event pairs.

Label Range	Definition	Example Event Pair
0.0–0.2	Unrelated; events concern different topics, entities, or timelines.	Will China invade Taiwan in 2024? vs. Karine Jean-Pierre out as Press Secretary by July 31?
0.2–0.4	Weakly related; minimal topical overlap, but no structural link.	U.S. military action against Iran in 2024? vs. Democrats win popular vote by 4–5%?
0.4–0.6	Moderately related; shared actors, parties, or contexts.	Will another candidate win NY-16 Democratic Primary? vs. Will a candidate from another party win NY Senate?
0.6–0.8	Strongly related; possible causal or strategic link.	Will Trump tweet 90+ times Oct 25–Nov 1? vs. Will Trump win 30% of Black men?
0.8–1.0	Highly related; one event entails the other.	Biden resign during his speech today? vs. Biden removed via 25th Amendment?

1120 H Heuristic Selection Methods

1121 To provide interpretable baselines for social opinion
1122 correlation reasoning, we introduce a set of
1123 heuristic scoring methods for ranking candidate
1124 event pairs. Unlike learned models, these heuris-
1125 tics use domain knowledge and surface-level at-
1126 tributes to estimate correlation scores without lan-
1127 guage understanding or reasoning. They serve as
1128 simple, zero-shot approximations to relevance or
1129 co-movement between social opinions.

1130 **Random** We assign a uniform random score to
1131 each candidate event. This provides a lower-bound
1132 reference for performance and reflects the difficulty
1133 of the task in the absence of any meaningful signal.

1134 **Volume-Based Sorting** We hypothesize that
1135 highly traded events are more likely to be central or
1136 influential in public discourse. For each candidate,
1137 we compute its total market trading volume (over
1138 the active time window) and use this as a relevance
1139 score. We experiment with two variants:

- 1140 • **Volume Max-to-Min:** Assigns the candidate’s
1141 normalized trading volume as its correlation
1142 score. Events with higher volume are assumed
1143 to be more generally relevant, independent of the
1144 base event.
- 1145 • **Volume Similarity:** Computes the absolute dif-
1146 ference in trading volume between the base and
1147 candidate events. Event pairs with more similar
1148 volumes receive higher scores, under the assump-
1149 tion that similarly salient events may co-occur
1150 in public discourse or exhibit social opinion co-

activation.

1151 **Temporal Overlap** We compute the degree of
1152 overlap in time between the base and candidate
1153 event windows. Events that occur in similar time-
1154 frames may be causally or contextually linked. The
1155 score is computed as the ratio of overlapping dura-
1156 tion to union duration.

1157 **Cross-Encoder Baseline** We include a
1158 strong neural retrieval baseline using the
1159 nli-deberta-v3-base cross-encoder. It jointly
1160 encodes event pairs and outputs a real-valued rele-
1161 vance score. Although trained on general-purpose
1162 sentence similarity or natural language inference
1163 tasks, it often captures surface-level lexical or
1164 semantic overlap, making it a competitive 0-hop
1165 semantic baseline.

1166 I Human Evaluation of Heuristic Scoring

1167 I.1 Setup

1168 **Objective and Sampling.** To assess whether our
1169 heuristic scoring function aligns with human intu-
1170 ition, we conducted an annotation study over 200
1171 event pairs. These pairs were drawn evenly across
1172 five correlation levels (very weak to very strong)
1173 according to the algorithmic relevance scores de-
1174 scribed in Section §4.2. This stratified sampling
1175 ensured that the full range of social opinion corre-
1176 lation strengths was represented, enabling consistent
1177 evaluation across relevance levels.

1178 **Annotators and Conditions.** Three annotators,
1179 who were NLP researchers involved in the project,
1180 participated in the study. While familiar with the
1181 modeling setup, they lacked domain-specific ex-
1182 pertise in forecasting or geopolitical reasoning. An-
1183 notations were conducted non-blind: annotators
1184 shared the same rubric and examples to guide their
1185 judgments

1186 I.2 Annotation Protocol

1187 **Rubric Development and Scoring Process.**
1188 Prior to annotation, the three annotators collabor-
1189 atively developed a shared rubric to define five
1190 levels of social opinion correlation, ranging from
1191 unrelated to highly related. This rubric was iter-
1192 atively refined through internal calibration rounds,
1193 ensuring that all annotators applied consistent se-
1194 mantic and causal reasoning. During annotation,
1195 each annotator independently rated all 200 event
1196 pairs on a continuous scale from 0.0 to 1.0 using
1197 the agreed rubric. Table 8 summarizes the scoring

Table 9: **Inter-annotator agreement.** Pearson correlation coefficients between annotators.

	Annotator A	Annotator B	Annotator C
Annotator A	1.000	0.840	0.739
Annotator B	0.840	1.000	0.794
Annotator C	0.739	0.794	1.000

bins and includes representative examples for each level.

Label Aggregation and Annotation Conditions. Although annotators shared a rubric, the annotation process itself was conducted independently without real-time coordination. Final labels were aggregated by majority vote; in cases of complete disagreement, we averaged the three scores. To prevent bias, annotators were shown only the event texts, without access to social opinion trajectories, model predictions, or algorithmic scores. This ensured that all judgments reflected semantic reasoning alone.

Annotator Agreement. We evaluate inter-annotator reliability using both pairwise Pearson correlations and intra-class correlation (ICC). As shown in Table 9, pairwise Pearson scores range from 0.739 to 0.840, indicating strong linear consistency among annotators. The highest alignment is observed between Annotators A and B (0.840), while A and C show slightly lower but still robust agreement (0.739). To complement this, we compute ICC(2,1) under a two-way random effects model, yielding a value of 0.777. This reflects substantial agreement across annotators and confirms the reliability of the human labels as a benchmark for model alignment.

I.3 Alignment with Heuristic Model

To measure how well the heuristic score $S(A, B)$ matches human judgment, we compute the Pearson correlation between model predictions and the aggregated human labels. The resulting correlation of $\rho = 0.697$ (Table 10) indicates strong alignment between the scoring function and human reasoning.

Table 10: **Model-human alignment.** Pearson correlation between the heuristic score and human annotations.

Method	Pearson Correlation
Heuristic score $S(A, B)$	0.697

J Detailed Performance Degradation After Cutoff

1233
1234

K Demo Interface Overview

1235
1236
1237
1238
1239
1240
1241

We build a web-based demo to showcase how our system connects real-time news and prediction market data. The interface allows users to explore forecastable events, understand model-generated reasoning, and vote on likely outcomes. Below, we walk through its key components.

Main Event Grid. Upon entering the demo (Figure 7), users see a grid of active prediction questions. Each card displays an event (*e.g.*, “Will X and Truth Social merger be announced before August?”) along with real-time probability estimates for each outcome (Yes/No), sourced from Polymarket. Users can filter events by domain (*e.g.*, politics, crypto) via the dropdown menu. Clicking on the “News” tab navigates to a dedicated news feed page. Selecting an individual event card leads to a detailed view for reasoning and voting.

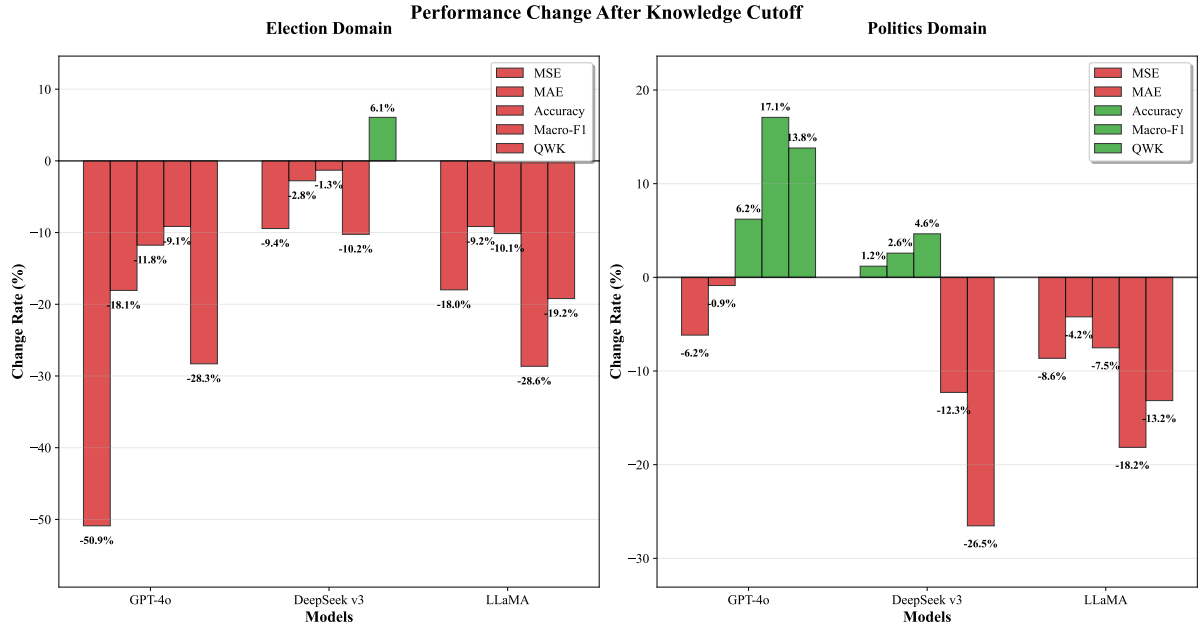
1242
1243
1244
1245
1246
1247
1248
1249
1250
1251
1252

News Integration. The “News” section (Figure 8) presents a chronological list of recent headlines. Clicking on any headline redirects users to the original article. Users can also expand or collapse a card by clicking the dropdown triangle on the right. When expanded, the card reveals any prediction events automatically identified as semantically or causally related to the article, bridging news and social opinion markets.

1253
1254
1255
1256
1257
1258
1259
1260
1261

Detailed Event View. When clicking on a grid cell, users are taken to a dedicated page for that prediction question (Figure 9). Here, they can select an outcome and choose from a list of candidate reasons generated by an LLM. These explanations help users interpret possible causal mechanisms. The right panel shows a time-series chart visualizing real-time market probabilities for each option. After selecting both an outcome and a reason, users can vote to register their social opinion.

1262
1263
1264
1265
1266
1267
1268
1269
1270
1271



Note: For MSE and MAE, values are sign-inverted for consistent interpretation. Positive values indicate performance improvement, negative values indicate degradation.

Figure 6: **Performance change after knowledge cutoff across domains and models.** Bars show the relative change in evaluation metrics on post-cutoff event pairs, compared to pre-cutoff ones. For metrics like MSE and MAE, values are sign-inverted to ensure a consistent interpretation, where negative values indicate degraded performance. GPT-4o shows a substantial decline across most metrics in the election domain, while performance remains more stable in the politics domain.



Figure 7: Main interface with real-time prediction events. Cards show current market probabilities and are filterable by topic.

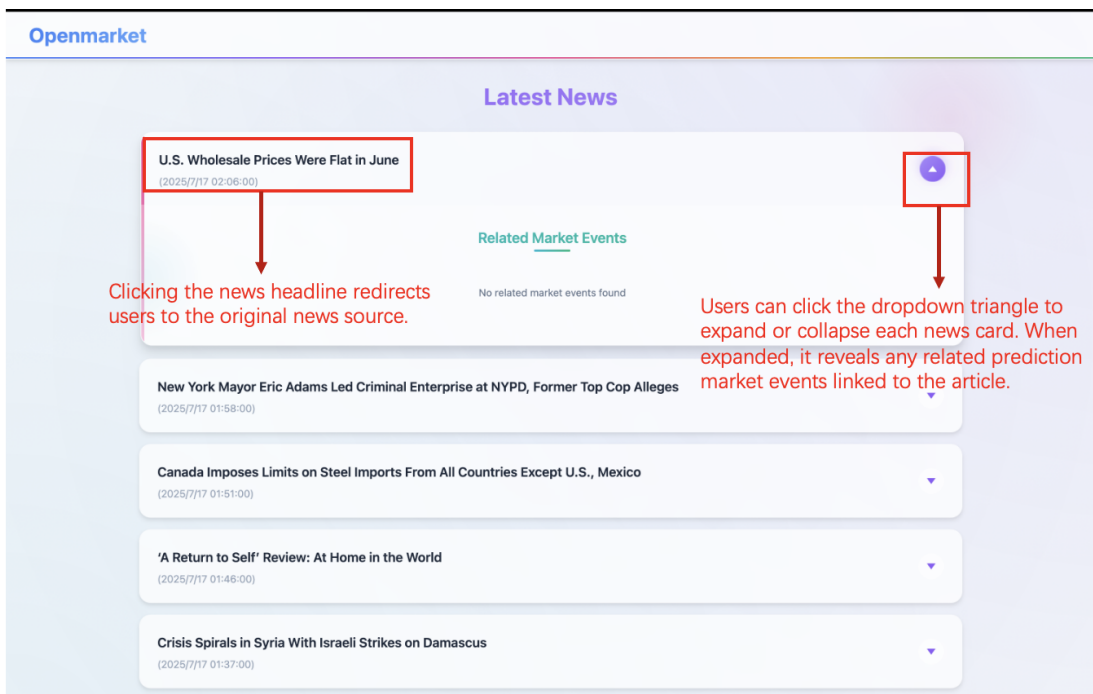


Figure 8: News page interface. Each news item links to the source and may surface relevant market events.

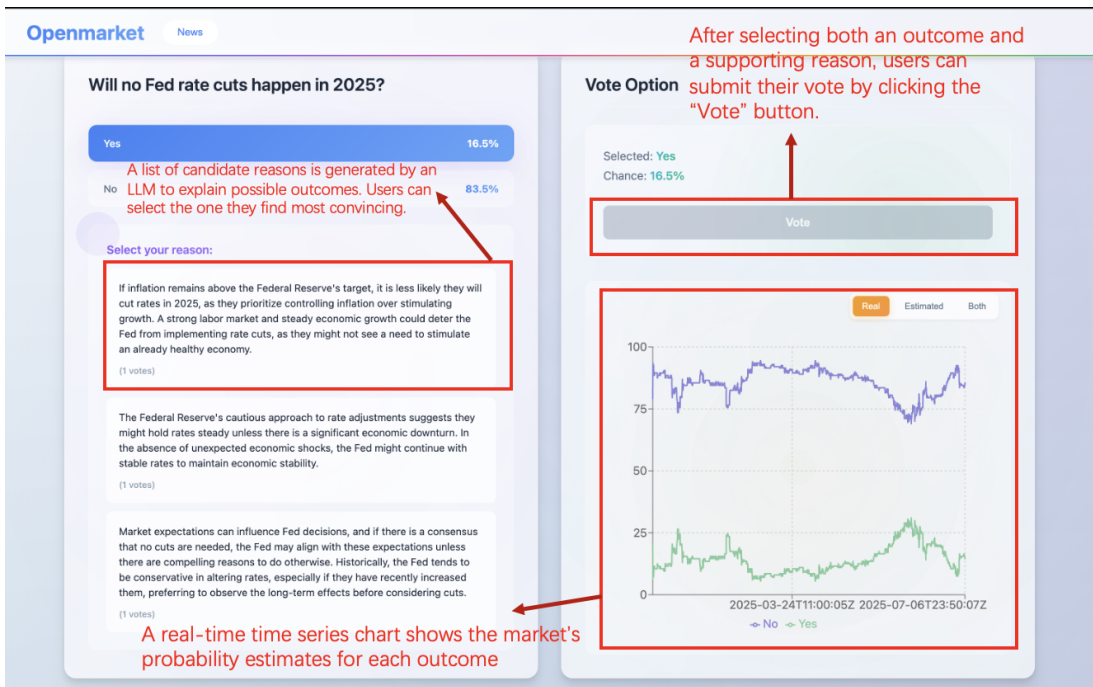


Figure 9: Detailed view of a prediction event. Users select an outcome and reason, then submit their vote.